

Chemical Bonding in Group III Nitrides

Aurora Costales,^{†,‡} Miguel A. Blanco,^{*,†} Ángel Martín Pendás,[†]
Anil K. Kandalam,[§] and Ravindra Pandey[§]*Contribution from the Departamento de Química Física y Analítica, Facultad de Química,
Universidad de Oviedo, 33006-Oviedo, Spain, and Department of Physics,
Michigan Technological University, Houghton, Michigan 49931*

Received October 24, 2001

Abstract: We analyze in this article the evolution of the chemical bonding in group III nitrides (MN, M = Al, Ga, In), from the N–N bond dominated small clusters to the M–N bond dominated crystals, with the aim of explaining how the strong multiple bond of N₂ is destabilized with the increase in coordination. The picture that emerges is that of a partially ionic bond in the solid state, which is also present in all the clusters. The covalent N–N bond, however, shows a gradual decrease of its strength due to the charge transfer from the metal atoms. Overall, Al clusters are more ionic than Ga and In clusters, and thus the N–N bond is weakest in them. The nitrogen atom charge is seen to be proportional to the metal coordination, being thus a bond-related property, and dependent on the M–N distance. This explains the behavior observed in previous investigations, and can be used as a guide in predicting the structures and defects on semiconductor quantum dot or thin film devices of these compounds.

1. Introduction

Group III (Al, Ga, and In) nitrides are gathering much attention from both the theoretical and experimental fields. The main reason behind this is their growing importance in the preparation of electronic devices.¹ Thus, the structural and electronic properties of the pure crystals of these compounds have been widely studied (see ref 2 and references therein). However, it is thin films, and not bulk crystals, that are used in electronic devices, and in these arrangements there is substantial disorder, with low coordination structures due to unsaturated bonds on the surface. To better understand these type of structures, finite clusters may be of help.³

In contrast to the wealth of results for the solid-state nitrides, studies on group III nitride clusters are scarce.^{4–8} Our group has conducted a series of DFT structural studies on these clusters,^{9–12} including some preliminary bonding results.¹⁰ The

picture emerging from these studies is clearly dominated by the existence of strong N–N bonds of multiple character, in the form of either N₂ units or N₃ azide-like units. This is very different from the bonding in the solid state, with 4-fold coordinated metals and nitrogens, and no N–N or metal–metal bonds. In the case of the clusters, Al–N bonded structures start to dominate at the trimer size, with a 2-fold coordination on both types of atoms. In the case of Ga and In nitride, however, preliminary results for (MN)_n clusters with n = 4, 5, and 6¹² indicate that N atoms without N–N bonding require at least three of the weaker Ga–N or In–N bonds. This requires a corresponding concentration of N atoms (either as N₂ or as N₃ units) in another part of the cluster when we consider stoichiometric clusters, suggesting that N segregation may occur during quantum dot or thin film deposition processes.

In this article, our aim is to explain how (or whether) the N–N bond weakens upon increasing the coordination of metals around the nitrogen. To accomplish this, we will study different series of clusters and compare them with the crystalline form to seek the emergence of bulklike bonding properties as the metal–nitrogen coordination increases. Particularly, we will address the bonding in three different ways: first, we will look at the bonding in terms of bond lengths and geometries; then, we will try to extract some bonding information from the relative energetic stabilities, that is, the binding; finally, we will use the Atoms in Molecules (AIM) theory to obtain atomic charges

* Corresponding author. E-mail: mblanco@mtu.edu. Temporary address: Department of Physics, Michigan Technological University, Houghton, MI 49931.

† Temporary address: Department of Physics, Michigan Technological University, Houghton, Michigan 49931.

‡ Universidad de Oviedo.

§ Michigan Technological University.

- (1) Nakamura, S. In *Proceedings of International Symposium on Blue Laser and Light Emitting Diodes*; Yoshikawa, A., Kishino, K., Kobayashi, M., Yasuda, T., Eds.; Chiba University Press: Chiba, 1996; p 119.
- (2) Serrano, J.; Rubio, A.; Hernández, E.; Muñoz, A.; Mújica, A. *Phys. Rev. B* **2000**, *62*, 16612–23.
- (3) Belyanin, A. F.; Bouilov, L. L.; Zhirnov, V. V.; Kamenev, A. I.; Kovalskij, K. A.; Spitsyn, B. V. *Diam. Relat. Mater.* **1999**, *8*, 369.
- (4) Langhoff, S. R.; Bauschlicher, C. W., Jr.; Pettersson, L. G. M. *J. Chem. Phys.* **1988**, *89*, 7354.
- (5) Nayak, S. K.; Khanna, S. N.; Jena, P. *Phys. Rev. B* **1998**, *57*, 3787.
- (6) BelBruno, J. J. *Chem. Phys. Lett.* **1999**, *313*, 795.
- (7) Timoshkin, A. Y.; Bettinger, H. F.; Schaefer, H. F. *J. Am. Chem. Soc.* **1997**, *119*, 5668.
- (8) Andrews, L.; Zhou, M.; Chertihin, G. V.; Bare, W. D.; Hannachi, Y. J. *Phys. Chem. A* **2000**, *104*, 1656.

- (9) Kandalam, A.; Pandey, R.; Blanco, M. A.; Costales, A.; Recio, J. M.; Newsam, J. M. *J. Phys. Chem. B* **2000**, *104*, 4361.
- (10) Costales, A.; Kandalam, A. K.; Martín Pendás, A.; Blanco, M. A.; Recio, J. M.; Pandey, R. *J. Phys. Chem. B* **2000**, *104*, 4368.
- (11) Kandalam, A. K.; Blanco, M. A.; Pandey, R. *J. Phys. Chem. B* **2001**, *105*, 6080–4.
- (12) Kandalam, A. K.; Blanco, M. A.; Pandey, R. *J. Phys. Chem. B* **2002**.

and bonding properties from the quantum mechanical calculations, by analyzing the topology of the electron density.

II. Computational Details

This article contains results from three types of systems, each one treated in a different but comparable way. First, in group III nitride clusters, the main subject of this report, we have used a procedure similar to the one outlined in ref 10, and we have also included results already presented in refs 9 and 10 (MN , M_2N_2 , and M_2N_2-2 clusters) to aid in determining the trends. Second, we have done calculations on N_2 and the N_2H_2 and N_2H_4 hydrides, to serve as a pattern of well-behaved triple, double, and single N–N covalent bonds. And third, we have also studied the crystals of the group III nitrides, as the infinite-limit of the cluster-growing process. We will describe each of these types of calculations in turn.

For the nitride clusters, the procedure begins with a DMol¹³ optimization of the desired structure. This is a Density Functional Theory (DFT) computational scheme, in which double- ζ numerical basis sets supplemented with polarization functions (DNP basis set) are used in a Linear Combination of Atomic Orbitals–Self-Consistent Field (LCAO–SCF) Kohn–Sham calculation. We have employed the Generalized Gradient Approximation (GGA) functionals of Becke¹⁴ and of Perdew and Wang¹⁵ to describe the exchange and correlation effects, respectively (BPW91). Numerical details of the SCF and symmetry-constrained optimization have been given elsewhere.⁹

To obtain analytical densities to perform Atoms in Molecules (AIM) calculations,¹⁶ we have performed single-point DFT–BPW91 calculations using 6-31G* basis sets within the Gaussian 98¹⁷ program (see ref 10 for a justification of the equivalence of the DMol and Gaussian basis sets). To make the comparison with the hydrides and crystals consistent, we have taken the Gaussian single-point and atomic energies to compute binding energies. As the final step in cluster calculations, we have used the AIMPAC95¹⁸ package to integrate AIM properties using the PROMEGA algorithm.

In the second type of systems, N_2 and N_2H_m hydrides, we have optimized the geometries directly with Gaussian, obtaining the bond properties with AIMPAC95. The structures used were the planar C_{2h} structure for N_2H_2 and the trans, also C_{2h} , structure for N_2H_4 . Both of them are the most stable structures at the level of theory employed, BPW91/6-31G*.

Although the experimental structure of the three group III nitrides considered is the hexagonal B4 structure, we have used the cubic B3 structure ($F43m$, with atoms in Wyckoff positions 4a and 4c), which is attainable as a metastable phase by epitaxial deposition. The B3 structure is more symmetric, with a single kind of M–N bonds, being thus better suited as a crystalline reference example. Both structures consist of vertex-sharing NM_4 tetrahedra, with different interplanar packings which affect only the third-nearest and further neighbor distances when comparing the ideal B4 structure, bearing the same relationship as the hcp and fcc structures in elemental solids. In the case of the MN B4 phases, the tetrahedra are almost regular, with nearest-neighbor distances of 1.86/1.90 (AlN), 1.94/1.946 (GaN), and 2.13/2.16 Å (InN).¹⁹ We have selected a B3 configuration equivalent to the experimental one by putting the volume per formula unit of the B3 phase equal to that of the B4, which gives nearest-neighbor distances of 1.888, 1.944, and 2.154 Å for Al, Ga, and In nitrides in the B3 phase, very close to the average B4 distance. We have performed

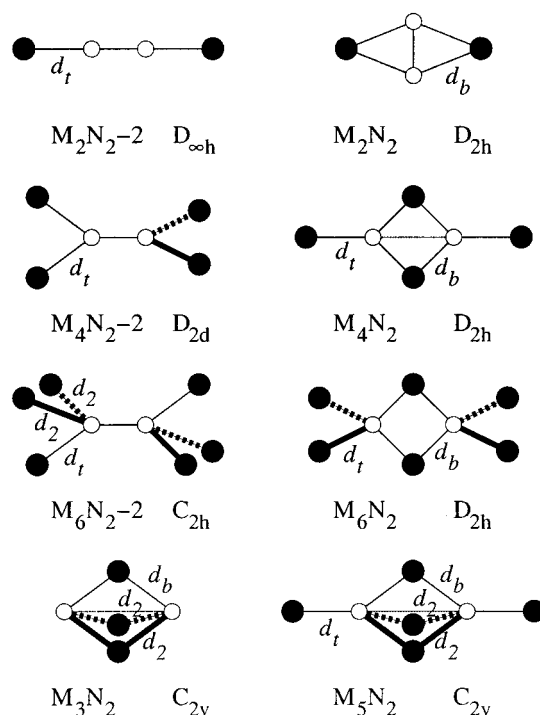


Figure 1. Schematic representation of the structures of M_mN_2 ($M = Al, Ga, In$) clusters. Large black circles represent metal atoms, small open circles are N atoms. Thick bonds come up from the plane, thick dashed bonds go below the plane. Thin dotted lines represent bonds that are present only for some compounds (see Subsection 3.4).

CRYSTAL95²⁰ BPW91 LCAO calculations for the three crystals at this experimental-like configuration, using the same basis set as in the molecular calculations to facilitate the comparison.²¹

III. Results

In this section, we will present the results of our calculations in three series of clusters, each one designed to test how the N–N bond behaves when its coordination increases in a different way. The first series, M_mN_2-2 series ($m = 2, 4, 6$), adds terminal metal atoms to N_2 , increasing the coordination while maintaining a N–N bond. Since the solid-state environment is tetrahedral, we have devised two further series of clusters: the edge-sharing tetrahedra M_mN_2 series ($m = 2, 4, 6$), with two bridge atoms, and the face-sharing tetrahedra M_mN_2 series ($m = 3, 5$), with three bridge atoms. Vertex-sharing tetrahedra configurations, although the most similar to the solid state, were ignored due to the extremely low symmetries they lead to. The structures used for these clusters are shown in Figure 1.

Despite the fact that the clusters are arranged in three series, we will present the results in a property-wise manner, leaving the discussion of the general trends in each series to the conclusions section. In the next subsections, we will first assess geometrical properties, followed by the study of the relative stabilities, then we will present the atomic charges, and we will conclude with the AIM bond properties.

A. Geometry. Table 1 presents the nearest-neighbor distances and binding energies per atom for all the clusters studied here.

(13) *Dmol user guide*, version 2.3.6. Molecular Simulations, Inc., 1995.

(14) Becke, A. D. *Phys. Rev. A* **1988**, *38*, 3098.

(15) Perdew, J. P.; Wang, Y. *Phys. Rev. B* **1992**, *45*, 13244.

(16) Bader, R. F. W. *Atoms in Molecules*; Oxford University Press: Oxford, 1990.

(17) **Gaussian 98**; Gaussian, Inc.: Pittsburgh, PA, 1998.

(18) Keith, T. A.; Laidig, K. E.; Cheeseman, J. R.; Bone, R. G. A.; Biegler-König, F. W.; Duke, J. A.; Tang, T.; Bader, R. F. W. *The aimpac95 programs*, 1995.

(19) Wyckoff, R. W. G. *Crystal Structures*; Interscience Publishers Inc.: New York, 1960; Vol. II.

(20) Saunders, V. R.; Dovesi, R.; Roetti, C.; Causà, M.; Harrison, N. M.; Orlando, R.; Zicovich-Wilson, C. M.; Torino, *Crystal95 user's manual*, 1995.

(21) The most diffuse exponents were reoptimized to avoid linear dependence, as is usual with CRYSTAL95 calculations.

Table 1. Interatomic Distances (\AA) of the Various Nitride Clusters under Study^a

cluster	d_h	d_t	d_b	d_2	E_{bind}
Al ₂ N ₂ -2	1.226	1.921			-2.885
Al ₄ N ₂ -2	1.571	1.871			-2.853
Al ₆ N ₂ -2	1.299	1.875		2.364	-2.361
Al ₂ N ₂	1.296		2.100		-3.083
Al ₄ N ₂	2.764	1.865	1.872		-3.222
Al ₆ N ₂	2.989	1.914	2.173		-2.852
Al ₃ N ₂	1.859		1.894	2.022	-2.842
Al ₅ N ₂	2.550	1.867	1.904	2.118	-3.011
Ga ₂ N ₂ -2	1.212	2.027			-2.840
Ga ₄ N ₂ -2	1.509	1.963			-2.786
Ga ₆ N ₂ -2	1.341	2.039		2.041	-2.635
Ga ₂ N ₂	1.274		2.201		-2.989
Ga ₄ N ₂	2.828	1.935	1.931		-2.952
Ga ₆ N ₂	3.194	1.957	2.292		-2.803
Ga ₃ N ₂	1.448		2.273	2.162	-2.634
Ga ₅ N ₂	2.342	1.884	2.122	2.122	-2.821
In ₂ N ₂ -2	1.197	2.286			-2.628
In ₄ N ₂ -2	1.438	2.165			-2.214
In ₆ N ₂ -2	1.347	2.295		2.308	-2.070
In ₂ N ₂	1.253		2.436		-2.750
In ₄ N ₂	3.101	2.134	2.144		-2.300
In ₆ N ₂	3.188	2.166	2.413		-2.253
In ₃ N ₂	1.412		2.476	2.374	-2.296
In ₅ N ₂	2.475	2.117	2.356	2.356	-2.260

^a Symbols are defined in Figure 1: d_h is the homonuclear nitrogen–nitrogen distance, d_t corresponds to terminal M–N bonds, d_b to bridge M–N bonds, and d_2 (when present) to the second kind of terminal or bridge M–N bonds. The last column gives the binding energy per atom (in eV).

Table 2. Evolution of the N–N Bond in the Hydride Series^a

molecule	d_h	E_{bind}/N	ρ_h	$\nabla\rho_h$
N ₂	1.116	-5.019	0.644	-2.076
N ₂ H ₂	1.257	-3.288	0.461	-1.056
N ₂ H ₄	1.503	-3.159	0.263	-0.386

^a Homonuclear N–N distance (d_h , in \AA), binding energy per atom (E_{bind}/N , in eV), and electron density (ρ_h , in electrons/Bohr³) and its Laplacian ($\nabla\rho_h$, in electrons/Bohr³) at the homonuclear bond point.

We will start focusing on the d_h (homonuclear N–N) distances, which will be compared with the corresponding distances for N₂ and N₂H_m hydrides included in Table 2. Looking at these distances, they can clearly be classified into different categories. First of all, N₂ gets a category by itself, with the shortest N–N distance of all. Then, M₂N₂-2, N₂H₂, and M₂N₂, with distances in the range 1.2–1.3 \AA . M₆N₂-2 have an intermediate distance, 1.30–1.35 \AA . M₃N₂, N₂H₄, and M₄N₂-2 share the range 1.45–1.55 \AA , with the exception of Al₃N₂, which has a longer distance of 1.86 \AA . All of the M₄N₂, M₅N₂, and M₆N₂ display much larger distances (>2.3 \AA).

These categories can then be naïvely labeled as having triple, double, single, and no N–N bonding, with the M₆N₂-2 having a very special place. However, it should not be implied that these clusters conform to the s and p covalent bonding scheme of, i.e., organic compounds or the N₂H_m hydrides used here as a pattern. To begin with, no Lewis configuration of shared electron pairs can be found to justify single bonds in M₃N₂, nor double bonds in M₂N₂, and M₆N₂-2 nitrogens will have a quite strange pairing scheme. To understand the bonding on these clusters, we cannot interpret M–N bonds as electron-pair covalent bonds, as we shall see later. N–N bonds can nevertheless be attributed an essentially covalent nature, owing to their nonmetal homonuclear character, whenever they exist. As to the existence of these bonds in edge- and face-sharing clusters, we will delay the discussion to Subsection III.D.

Table 3. B3 Phase Crystal Properties^a

crystal	AlN	GaN	InN
a	4.360	4.489	4.974
d	1.888	1.944	2.154
E_{bind}/N	-5.559	-3.155	-3.762
Q_N	-2.387	-1.615	-1.492
f_N	0.788	0.571	0.478
ρ	0.075	0.102	0.084
$\nabla^2\rho$	0.458	0.382	0.303
r^N	1.114	1.027	1.060
r^M	0.774	0.916	1.094

^a Lattice parameter (a), nearest-neighbor distance (d), and nitrogen radius along the bond direction (r^N) in \AA , nitrogen atomic charge (Q_N) in electrons, and bond point electronic density (ρ) and Laplacian ($\nabla^2\rho$) in atomic units. E_{bind}/N is the binding energy per atom (in eV). f_N is the volume fraction occupied by the N atom.

Before comparing the M–N distances of the different clusters studied, we should present the two end-limits of M–N bonding. On one hand, as presented in refs 9 and 10, MN diatomic molecules have distances of 1.82, 2.06, and 2.28 \AA for M = Al, Ga, and In, respectively, with AIM charges of 0.9 e for Al and around 0.5 for Ga and In, resulting in a partially ionic bonding. On the other extreme, the MN B3 experimental-like (see Section II) crystals show a tetrahedral environment for both M and N. The geometric, energetic, and bonding properties of these crystals are presented in Table 3. As can be seen, the AIM charges are larger, giving rise to a more ionic bonding, whereas the distances are smaller than those in the diatomics except for AlN. This can be understood comparing the atomic radius in the bond direction (r^N and r^M in Table 3, d_N and $d - d_N$ in Table 3 of ref 10): both the N and the M radii decrease in forming the GaN and InN solids, whereas the Al radius remains constant and the N radius increases in forming the AlN solid. This may be due to the high negative charge of the N atom in the solid, tending to increase its radius.

To discuss the M–N distances in Table 1, it is best to sort them into two categories: terminal M–N bonds, listed in column d_t , and d_2 for the second M₆N₂-2 distance, and bridge M–N bonds, listed in column d_b and the remaining entries of column d_2 . Let us start with terminal M–N bonds. These bond lengths cluster around the MN B3 solid and diatomic distances, with Al_mN_n distances being the shortest, followed by Ga_mN_n, and with In_mN_n having the longest terminal M–N bonds. The only exceptions to this ordering are Ga₅N₂, with a somewhat shorter Ga–N bond than the other compounds, and the second kind of Al–N distances in Al₆N₂-2, much larger than the other. M₅N₂ terminal bonds are in fact among the shortest for each metallic element, together with the M₄N₂, while both M₆N₂-2 M–N bonds are the longest. However, whereas both types of M–N bonds have almost the same length in Ga₆N₂-2 and In₆N₂-2, they are very different in Al₆N₂-2.

The unexpected behavior of M₆N₂-2 clusters, with N–N distances between those of M₂N₂-2 and M₄N₂-2 clusters and longer M–N distances, deserves some further attention. As previously stated, N atoms usually form only three covalent bonds, except when they act as a Lewis base and share its remaining lone electron pair. This is not the case for these clusters, since the N atoms carry a significant negative charge as we shall see in the next subsection. In addition, the N–N bond has a distance shorter than those corresponding to single bonds, indicating a considerable double bond character. Particularly for Ga₆N₂-2 and In₆N₂-2, these clusters can be

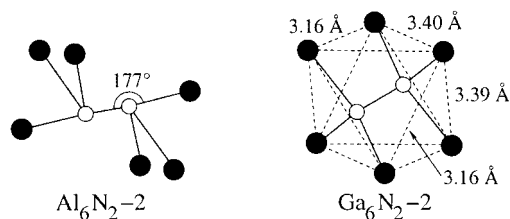


Figure 2. Optimized geometry of Al_6N_2-2 and Ga_6N_2-2 .

considered as a N_2 molecule accepting charge transfers from a set of metal atoms, and thus increasing its N–N distance, but forming very weak bonds with them, explaining the longer M–N distances. In fact, the Ga and In atoms show an almost regular octahedral structure, with the N_2 molecule inside (see Figure 2). The distances between metal atoms are, however, too large to be considered as bonded: 3.15–3.39 and 3.61–3.80 Å for the Ga and In clusters, respectively, whereas the distances for the M_2 cluster/M metallic solid are 2.80/2.44 and 3.17/3.25 Å for $\text{M} = \text{Ga}$ and In , respectively. Thus, the metal atoms can be regarded as having a nondirectional bond with N_2 , and packing around it in the least interaction geometry, an octahedron. In the case of Al_6N_2-2 , however, the N_2 molecule is too large to fit inside an octahedron of noninteracting Al, and thus the preferred structure (see Figure 2) resembles that of a Al_2N_2-2 cluster, almost linear and with similar distances, with two long-distance M–N bonds on each N atom that leave an almost equilateral (the unique angle is 61.3°) Al triangle at each end of the molecule. The Al_6 geometry is that of an octahedron enlarged along one of its S_3 axes, with the nitrogen molecule oriented along one of the former C_4 axes and further displacing both triangles. The existence of a linear Al–N–N–Al unit indicates that this is not just a steric effect, but that also electronic structure preferences play some role here.

With respect to the bridge M–N bond distances, the main trend is again to sort themselves by the metallic atom involved, with the Al–N distances being generally smaller than those of Ga–N, and these in turn smaller than those of In–N. However, there are several exceptions to this trend, the most important being that of the M_4N_2 clusters, with a much shorter bridge bond length than all other metallic bridge atoms, on the order of magnitude of terminal bonds. All the other bridge distances tend to be larger than terminal distances, and they have a much wider range of values. Thus, although bridge atoms should be the metallic atoms closer to the solid-state behavior, the tendency to form N–N bonds puts a lot of stress into these bonds. The N–M–N bond angles are around 30° for M_2N_2 and M_3N_2 (except Al_3N_2 , around 55°), corresponding to a short N–N distance. They are around 65° for M_5N_2 (again except Al_5N_2 , around 84°), corresponding to long-range N–N bonding. Finally, the angles are close to 90° for M_6N_2 ($<90^\circ$) and M_4N_2 ($>90^\circ$), making an almost perfect square. It should be kept in mind that, were the environment around the N atoms a perfect tetrahedron, the M–N–M angle would be around 70° for edge-sharing and around 39° for face-sharing tetrahedra. The actual values are either much smaller or much larger than these, except for Ga_3N_2 and In_3N_2 , indicating a clear departure from the tetrahedral environment in all but these two compounds. In fact, even in these two compounds the similarity is fortuitous, since there is a quite clear covalent N–N bond, as we shall show in Subsection III.D.

B. Stability. The last column of Table 1 contains the binding energy (E_{bind}) per atom of all M_mN_n clusters. The binding energy, being defined as the total energy of the cluster minus that of the separate atoms, is obviously larger for clusters of bigger sizes. To ease the comparison of the relative stabilities of the differently sized clusters, the binding energy per atom is commonly used. However, this magnitude cannot be used in thermodynamic relations, and should not be considered as an indication of bond strength but of overall stability. As was expected, the largest E_{bind} per atom values correspond to the N_2 molecule, N_2H_m hydrides (see Table 2), and the B3 MN crystals (see Table 3). In the first two cases, the stability is probably coming from the strong covalent bonding, whereas the B3 crystals, with a bonding quite similar to that of the M_mN_n clusters, as we shall see, has nevertheless all tetrahedral valences of N and M atoms saturated, bringing a tighter binding for each. It is important to remember that the diatomic MN molecules (with binding energies per atom of -1.307 , -1.196 , and -1.001 eV for $\text{M} = \text{Al}$, Ga , and In) are by far the clusters with lower overall stability, corresponding to minimal coordination. Among the clusters, Al ones are usually more stable, followed by Ga and then In. Al_6N_2-2 has an exceptionally low binding energy, and Ga_6N_2-2 and In_6N_2-2 are also among the less stable clusters, indicating the very weak overall bonding of the six metal atoms to the inner N_2 molecule.

An interesting concept arises if we focus on the number of bonds in each structure. If, instead of dividing E_{bind} by the number of atoms in the cluster, we calculate the binding energy per bond, counting as such those in the conventional skeleton of the molecule depicted in Figure 1, we will get a better measure of the average strength of the bonds of each cluster. This completely changes the picture. There is still an overall ordering Al/Ga/In, and N_2 and N_2H_2 , with strong covalent bonds, are the ones with a larger stabilization per bond. However, the B3 phase crystals, with four bonds per unit formula, show in fact the weaker bonds in GaN and InN, and only an intermediate strength bond in AlN. This may be explained as a consequence of the larger ionic character of the crystals when compared with the clusters, with the Al–N bond being stronger because of the larger charge transfer (see the next subsection): the Coulomb binding energy is proportional to the square of the ionic charge, and inversely proportional to the nearest-neighbor distance.

A clearer order is also established among the clusters: M_2N_2-2 and M_4N_2-2 , in this order, are the clusters with larger binding energies per bond, corresponding to short N–N distances accompanied by short M–N distances. Then come the M_6N_2-2 clusters, with short N–N bonds and intermediate M–N ones, except for Al_6N_2-2 , which has a very long M–N distance and a lower binding energy per bond. M_4N_2 and M_6N_2 come next, with short M–N distances and no N–N interaction. Finally, M_2N_2 , MN, M_5N_2 , and M_3N_2 show the lowest binding energies per bond of the M_mN_n clusters. M_2N_2 clusters have a very strong and short N–N bond, but also four very long, weak M–N bonds, which lower the average binding energy. MN diatomics still show a weak bond when compared with the previous clusters, to which no clear explanation has been found. Finally, M_5N_2 and M_3N_2 show very strained N–N and M–N interactions due to their crowded coordinations, showing also quite long M–N bonds.

Table 4. AIM Atomic Charges (in electrons)^a

cluster	Q_N	Q_{M_t}	Q_{M_b}	Q_{M_2}
Al ₂ N ₂ -2	-0.644	0.641		
Al ₄ N ₂ -2	-1.561	0.782		
Al ₆ N ₂ -2	-1.746	0.547		0.602
Al ₂ N ₂	-0.794		0.794	
Al ₄ N ₂	-2.220	0.787	1.434	
Al ₆ N ₂	-2.389	0.796	0.800	
Al ₃ N ₂	-1.583		1.285	0.940
Al ₅ N ₂	-2.348	0.821	1.317	0.869
Ga ₂ N ₂ -2	-0.456	0.457		
Ga ₄ N ₂ -2	-1.068	0.536		
Ga ₆ N ₂ -2	-1.154	0.337		0.409
Ga ₂ N ₂	-0.526		0.526	
Ga ₄ N ₂	-1.471	0.577	0.895	
Ga ₆ N ₂	-1.612	0.536	0.541	
Ga ₃ N ₂	-0.837		0.589	0.541
Ga ₅ N ₂	-1.446	0.692	0.508	0.502
In ₂ N ₂ -2	-0.376	0.378		
In ₄ N ₂ -2	-0.939	0.470		
In ₆ N ₂ -2	-0.972	0.313		0.332
In ₂ N ₂	-0.476		0.477	
In ₄ N ₂	-1.374	0.545	0.830	
In ₆ N ₂	-1.512	0.516	0.485	
In ₃ N ₂	-0.772		0.546	0.499
In ₅ N ₂	-1.343	0.615	0.472	0.495

^a The symbols *t*, *b*, and 2 stand for metal atoms which connect to N through the corresponding bond (see Figure 1 and Table 1).

C. Atomic Charges and Ionicity. For the discussion of ionicity we have selected AIM atomic charges. Other schemes (e.g., Mulliken) produce different values for the charge, although the trends, our main focus in this paper, are very similar. Moreover, Mulliken charges are very sensitive to the details of the calculation, whereas AIM charges, derived from the electronic density, are molecular-orbital independent and consistent across series of compounds. The AIM charges for all the clusters studied are gathered in Table 4. As a reference, charges for the B3 crystal atoms are also included in Table 3, and the atomic charges computed for the MN diatomic molecules in ref 10 were 0.919, 0.542, and 0.528 for the Al, Ga, and In atoms, respectively. Looking at the charges of the N atoms in the diatomics, clusters, and solid, it is easy to conclude that they depend mainly on the coordination number. Roughly speaking, the more M atoms surrounding a N atom, the more charge that is transferred to it, in an amount that seems to be very similar for each new M atom in the N coordination sphere. Thus, M₆N₂ clusters show the highest N charges for M = Al, Ga, and In, with values almost equal to those of the B3 phase, as the tetrahedral coordination of N would suggest. These charges are very high, indicating a very ionic bonding, especially in the case of AlN and Al₆N₂. After these, the N atoms in M₅N₂ follow, having a similar charge to the 3-fold coordinated M₄N₂, probably because of the strain in the face-sharing environment. This also lowers the charge of the M₃N₂ clusters, with a 3-fold coordination but a face-sharing environment. M₂N₂ and M₂N₂-2 have the smallest charges, in agreement with their M atoms loosely bound to a tightly bonded N₂ unit. The charge transfer also grows with coordination in the M_mN₂-2 series, but the increase is very small in going from the strong M–N bonds of the *m* = 4 case to the weak M–N and strong N–N bond of *m* = 6. It should be noticed that, although the N–N bond counts toward the coordination number value, it does not involve any charge transfer (both nitrogens are equivalent by symmetry),

and so the M₄N₂-2 N charge is in agreement with a coordination number of 2, despite the 3-fold coordination of the N atom.

With respect to the charge on the metallic atoms, a clear distinction should be made between terminal and bridge atoms. In the first case, with coordination 1, the charge transfers are moderate compared to both B3 and MN diatomics, specially in the case of Al. Again, charge transfers are larger for Al than for Ga and In, but the difference is not so high as in the limiting cases of diatomics and crystals. M₅N₂ terminal atoms have the largest charges for a given M atom, and there is a trend to decrease with the M–N distance in Ga and In, which has several exceptions in the case of Al. Overall, the charges on the terminal atoms of M₆N₂-2 and M₂N₂-2 are the lowest, due to the small charge acceptance of their strongly bonded N₂ units.

Focusing now in the charges of bridging metal atoms, we again see a clear separation of the charge transfers by which Al atoms get larger charges than Ga and In, in this order. Within a series of clusters sharing a common metal atom, charges are fairly constant (0.79 to 0.94 in Al, 0.50 to 0.58 in Ga, and 0.47 to 0.54 in In compounds). The main exceptions are M₄N₂ clusters, and the highly distorted third bridge atom of Al₅N₂ and Al₃N₂, which have much larger charges and also a correspondingly lower distance.

The charge transfers in these clusters show a very polar type of bonding, with an important ionic component. Overall, it seems that each M–N bond has a charge transfer that depends mainly on the metal atom involved (around 0.8 electrons in Al, and around 0.5 electrons for Ga and In, as the diatomic molecules seem to suggest), but which is also modulated by distances, being larger for the lower distance bonds. Given the usual rigidity of both bond distances and angles in covalent tetrahedrally bonded compounds (with angles of 109.5°), our attribution of a low covalent character to the M–N bond is also supported by the bond angles about the N atoms: 75° for Al₆N₂-2 and around 150° for M₄N₂-2 in terminal bonds, around 90° for edge-sharing bridging in M₄N₂ and M₆N₂ and also in face-sharing bridging in M₅N₂, whereas it is split between 100° and 125° in the two different angles of M₃N₂ compounds. M₂N₂ M–N–M angles are ≈150°. The only clusters having a seemingly tetrahedral coordination for N are Ga₆N₂-2 and In₆N₂-2, with angles ranging from 108° and 112°, but as we have seen previously this fact is to be attributed to the almost octahedral arrangement of the M atoms weakly bonded to a strong and small N₂ unit. Also, the wide range of distances for each type of bond is additional evidence against covalent bonding.

An interesting fact arises when comparing the bond charge transfers: the bridging atoms in M₄N₂ show a charge almost double that of the terminal atoms, supporting the idea of fixed charge transfers per bond, but this does not happen in M₆N₂, M₅N₂, and M₃N₂. This seems to be related to a saturation of charge in the N atoms: the bridge atoms in M₆N₂ cannot donate more charge to the N atoms, because Q_N has already reached the value of the bond-saturated B3 structure. Furthermore, this maximum acceptable charge depends on the nature of the M atom, and is thus linked to the electronegativity difference. This saturation effect also appears in the M₅N₂ clusters. The M₃N₂ case is more complicated, since all bridging atoms get a charge larger than the average terminal atom, but not as large as in

Table 5. AIM Bond Properties^a

cluster	ρ_h	$\nabla^2\rho_h$	r_t^N	r_b^N	r_2^N
Al ₂ N ₂ -2	0.475	-1.050	1.119		
Al ₄ N ₂ -2	0.212	-0.109	1.102		
Al ₆ N ₂ -2	0.401	-0.752	1.086		1.422
Al ₂ N ₂	0.422	-0.792		1.247	
Al ₄ N ₂	0.044	+0.059	1.096	1.097	
Al ₆ N ₂	(0.024)	(0.043)	1.126	1.293	
Al ₃ N ₂	0.119	+0.152		1.111	1.197
Al ₅ N ₂			1.099	1.121	1.261
Ga ₂ N ₂ -2	0.492	-1.109	1.055		
Ga ₄ N ₂ -2	0.249	-0.228	1.036		
Ga ₆ N ₂ -2	0.379	-0.703	1.070		1.071
Ga ₂ N ₂	0.446	-0.910		1.149	
Ga ₄ N ₂	(0.040)	(0.103)	1.018	1.011	
Ga ₆ N ₂	(0.018)	(0.036)	1.026	1.191	
Ga ₃ N ₂	0.299	-0.367		1.171	1.131
Ga ₅ N ₂	0.044	+0.178	0.979	1.112	1.112
In ₂ N ₂ -2	0.513	-1.216	1.109		
In ₄ N ₂ -2	0.289	-0.359	1.062		
In ₆ N ₂ -2	0.359	-0.588	1.120		1.140
In ₂ N ₂	0.467	-1.012		1.188	
In ₄ N ₂	(0.029)	(0.082)	1.045	1.045	
In ₆ N ₂	(0.016)	(0.036)	1.057	1.182	
In ₃ N ₂	0.325	-0.462		1.197	1.162
In ₅ N ₂	0.034	+0.120	1.024	1.154	1.154

^a Electron density (ρ_h , in electrons/Bohr³) and its Laplacian ($\nabla^2\rho_h$, in electrons/Bohr⁵) at the N–N middle points, and distances from nitrogen to the heteronuclear bond points (r^N , in Å). *t*, *b*, and 2 subscripts stand for terminal, bridge, and a second kind of terminal or bridge M–N bond, respectively. Numbers in parentheses correspond to ring critical points, not bonds.

M₄N₂ bridge atoms. This may be related to the strained geometry of these clusters.

D. AIM Bond Properties. To analyze the bond properties in all the systems studied here, we will now focus on the topological features of their electron density in light of the AIM theory.¹⁶ Assuming that chemical bonds are identified with gradient paths connecting bond points with two adjacent nuclei, the chemical graphs of the clusters studied here are showing the structure depicted in Figure 1. Atom-connecting lines in that figure correspond to AIM bonds, with the only exception being N–N bonds plotted with a thin dotted line (M₄N₂, M₃N₂, and M₅N₂). From these N–N connections, the only ones corresponding to AIM N–N bonds are those of Al₄N₂, all M₃N₂, and all M₅N₂ except for Al₅N₂. Of these, only Ga₃N₂ and In₃N₂ correspond to short distance N–N bonds, with the rest of them being critical points due to symmetry or special geometric arrangements, and corresponding to strained situations.

Table 5 presents the electronic density and its Laplacian, and the distance to the N nucleus, of the different bond points of the clusters studied here. The strained character of the N–N bonds in Al₄N₂, Al₃N₂, Ga₅N₂, and In₅N₂ is supported by their low densities and positive Laplacians, uncommon for the usually strong and covalent N–N bonds.

The evolution of the N–N bond in the three different series of compounds can be addressed now. First, in the M_nN₂-2 series the bond is strong (high density) and clearly covalent (large, negative laplacian) for the *n* = 2 clusters, weaker and far less covalent (smaller densities and laplacians) for *n* = 4, and again stronger and covalent for *n* = 6, in agreement with our previous distance-based discussion. Second, the M_nN₂ edge-sharing series shows a strong N–N bond in the *n* = 2 cluster, but for the *n* = 4 clusters this is gone, except for the very weak bond in Al₄N₂, whereas the symmetry-forced critical point is a ring point in

all other *n* = 4 and 6 clusters. Finally, in face-sharing configurations, Ga₃N₂ and In₃N₂ have strong covalent N–N bonds, with densities intermediate to those of double (N₂H₂) and single (N₂H₄) ordinary N–N bonds. However, Al₃N₂, Ga₅N₂, and In₅N₂ only show a residual (long distance, low density, and positive Laplacians) N–N bond, and Al₅N₂ does not display it. Overall, it seems that at least 3-fold metal coordination around N is needed for the N atoms to be separated, and that Al–N bonds are the ones with a better chance of achieving this separation (the Al₄N₂ bond point, a symmetry-forced critical point, has the longest distance for a N–N bonding interaction, and is probably spurious). This is confirmed in our calculations of M₃N₃ clusters, reported elsewhere.¹¹

Regarding the M–N bonds, we find that all of them show small electron densities (lower than 0.1 e/bohr³) and positive Laplacians, on the same order of magnitude as the B3 phase ones. This supports the picture of a very ionic type of bonding, rather than a shared-electron covalent one, reinforcing what we already found in the previous subsection. Both densities and Laplacians can be seen to depend mainly on the distance from the bond point to the nucleus of either atom, r^N and r^M , decaying exponentially as we showed in ref 10.

Other important points regarding ρ are that, for terminal M–N bonds, the larger densities correspond to Ga compounds, then to In, and finally to Al, except for the MN (see ref 10) and M₂N₂-2 molecules, where the Al–N bond has a larger density than the In–N bond. This trend is also displayed by the B3 solid results (Table 3), and can be explained in terms of Pauling's electronegativities: Ga has the larger one, and thus should have the most covalent M–N bond in the series, with the largest ρ_t , followed by In, and finally Al, with a large charge transfer to help deplete electron density from the bond region, will be the one with the lowest ρ_t .

The deformation of the N atom is seen to be most similar to the B3 phase in the M₄N₂ clusters. Looking at the r^N distances to the M–N bond points of M₄N₂, M₆N₂, and M₅N₂, the only clusters with a more or less *closed* environment surrounding N, M₄N₂ is the only one in which nitrogen extends the same distance in both terminal and bridging bonds, and it is the closest to the B3 radius for them. It is also on these M₄N₂ clusters that the M atoms behave in the same way with respect to each M–N bond, with the bridge atoms getting a double share of charge because of the two M–N bonds, and thus each bond has both a similar charge transfer and a similar r^N value when comparing bridge and terminal bonds, and these properties are also similar to those in the B3 solids. This is not the case in the other two clusters: in M₆N₂, bridge atoms get more or less the same charge as terminal atoms, and thus almost half of the charge-transfer per bond and a different r^N value. The same happens in all M₅N₂ clusters except for Al₅N₂, in which one of the bridging atoms seems to get a double share of charge, and the r^N for this atom is correspondingly similar to that of the terminal bond and to that of the B3 phase. A behavior similar to that of the M₅N₂ clusters is observed in the M₃N₃ clusters.

The similarity between the M–N bonds of M₄N₂ and the MN B3 phase can be further confirmed in Figure 3. There, the laplacian of Al₄N₂ and of the three B3 crystals is plotted, along with the bond lines (thick) and the atomic basin limits (dotted thick). The basin limits, defining r^N and controlling the charge, are very similar in shape to those of the B3 phase near the M–N

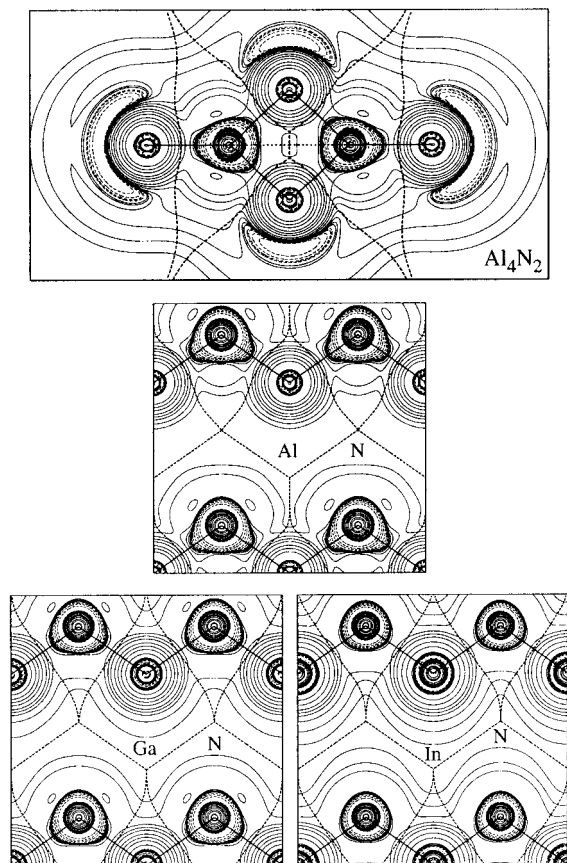


Figure 3. Laplacian of the electron density (thin lines), bond lines (solid thick lines), and atomic surfaces (dotted thick lines) for Al_4N_2 and the AlN , GaN , and InN crystals. The plots of Al_4N_2 and AlN use the same distance scale, whereas the scales for GaN and InN differ.

bond point, the most important accumulation of charge in the valence region. The polarization of the charge accumulation regions of N (dotted lines, negative Laplacian values) toward the three Al atoms resembles the tetrahedral distortion in the solid. The main difference lies in the large charge accumulation regions behind the four Al atoms, opposite to the Al–N bonds: the Al atoms, with only one or two N atoms on their coordination spheres, still conserve part of their valence shell, with the nitrogens accepting only part of it. This happens in all Al clusters, but not for Ga and In, whose more diffuse outer valence shells do not have charge accumulation regions in their Laplacians. In contrast with this unsaturated Al behavior, the Al (and also the Ga and In) atoms in the B3 structure have completely lost their valence shell, appearing as almost spherical ions in the crystal.

When comparing AlN , GaN , and InN crystal Laplacians, an interesting feature can be seen: Al, the smallest cation in the series, is the least distorted from a sphere, followed by Ga, and then In. In contrast, N is most deformed in AlN , less so in GaN , with InN having the least distorted N atom. This correlates very well with the relative volumes of the two species in each crystal: N is far larger than Al in AlN , comprising almost 80% of the volume, and thus has a larger deformability; N is still larger than Ga in GaN , with 67%, and just smaller than In in InN , with 48% of the volume. In this last crystal, the deformations of the In and the N laplacians seem almost of equal extent at first sight.

IV. Summary and Conclusions

The evolution of the chemical bond in group III nitride clusters has been studied in comparison to that in N_2 hydrides and MN crystals by means of DFT-GGA calculations and AIM analysis. In particular, we have shown how the N–N bond is gradually weakened in the $M_n\text{N}_{2-2}$ series in a way very similar to that in the hydrides, with the exception of the $M_6\text{N}_{2-2}$ clusters. These clusters have a smaller binding energy, with a N_2 molecule weakly bonded to the six M atoms. In the case of the edge-sharing series, 3-fold coordination proved to be enough to sustain a configuration without the N–N bond, whereas in the face-sharing series the N–N bond, when it exists, is in a strained configuration. Regarding the energy per bond, it shows that although the MN crystals have a greater overall stability than the clusters, it is only due to the higher coordination: the M–N bond is even weaker than the N–N bonds which can be labeled as single. The only reason behind the stabilization of structures without N–N bonds is the increase in coordination.

While the N–N bond is always of a covalent type, the M–N bonds show a considerable ionic character in all of the clusters, with the crystal structures having the higher ionicity. The overall charge transfer is larger for Al compounds than for Ga and In compounds. The charge on the N atoms is proportional to the metal coordination about them, but once it achieves the crystalline value it seems to saturate. In all cases, the charge transfer is related to the bonds, and is larger for shorter distances. Thus, the shorter and stronger M–N bonds are also those displaying larger bond charge transfers.

The atomic basins and the Laplacian of the electron density near the atoms are also deformed proportionally to the charge transfer. The $M_4\text{N}_2$ clusters, with similar charge transfers in the three bonds of each nitrogen and total nitrogen charge very similar to the crystal one, show the nitrogen more like the solid-state atom. The largest atomic deformations appear in the Al–N bonds, much larger than in Ga–N and In–N bonds, and this is related to the relative volumes. Finally, Al retains part of its valence shell, as displayed by the Laplacian of the electron density, both coordinations one and two, but it loses that shell in the solid, with coordination four, the system with the largest Al charge in this study.

Overall, it is seen that, while the N–N bond leads to a larger stabilization of the system, increasing the coordination of the N atom by having a larger number of weaker M–N bonds can stabilize the system in configurations lacking N–N bonds. This explains the behavior previously observed, for which the smaller clusters, with a low coordination, display structures dominated by the N–N bond. Stoichiometric clusters of larger sizes still show this kind of structure in GaN and InN clusters, whereas in AlN clusters the Al–N bond overcomes the N–N bond for a rather small size (trimers): this agrees with our present results, for which the Al–N bond is seen to be much stronger than Ga–N and In–N bonds. Our finding that a high coordination is necessary to avoid N–N bonds allows us to predict the existence of structures with higher local concentration of metal atoms, bonded to a single N atom, coexisting with regions of correspondingly higher local nitrogen concentration dominated by N–N bonds, as those displayed by our preliminary results for larger stoichiometric GaN and InN clusters. Since the

molecular beam epitaxy methods used in the quantum dot or thin film deposition proceed layer by layer, in a low coordination environment, it is expected that N–N bonded defect structures leading to N segregation occur. These microscopic features may well propagate macroscopically as the electrical or optical properties of the devices are concerned, and so further attention on the basic experimental and applied materials science fields should be directed at this issue.

Acknowledgment. Funding from the Spanish DGICYT grant BQU2000-0466 is acknowledged. M.A.B. and A.C.C. wish to thank NATO, the Spanish MEC, and the Principado de Asturias CEC for scholarships supporting their stay at Michigan Technological University. A.K. and R.P. thank Accelrys Inc. for the support of this study.

JA0173800